ISSN 0036-0244, Russian Journal of Physical Chemistry, 2006, Vol. 80, Suppl. 1, pp. S14–S20. © Pleiades Publishing, Inc., 2006.

STRUCTURE OF CHEMICAL COMPOUNDS, INCLUDING CONDENSED MEDIA

Atom–Atomic Potentials and the Correlation Distribution Functions for Modeling Liquid Benzene by the Molecular Dynamics Methods

T. V. Bogdan

Faculty of Chemistry, Moscow State University, Leninskie gory, Moscow, 119992 Russia

E-mail: bogdan@ioc.ac.ru

Received February 14, 2006

Abstract—A brief review of the potential functions used in the molecular dynamics modeling of liquid benzene is presented. The structural characteristics of liquid benzene obtained from the correlation distribution functions are discussed. It is demonstrated that, within the framework of this approach, the predicted structure of liquid benzene is virtually independent of the form of the potential used.

DOI: 10.1134/S0036024406130036

Numerical modeling is one of the modern approaches to studying the structure of liquids. To realize this method, it is necessary to construct an interaction potential capable of predicting the microscopic and macroscopic characteristic of the liquid. It is believed that liquids can be most effectively described with the help of distribution functions, since this treatment makes it possible to determine the thermodynamic parameters of the liquid from distribution functions obtained by computer simulations [1]. Thus, the approach described in [1] implies that there is an unequivocal relationship between the interaction potential and the structure of the liquid. In the present work, we briefly review the existent interaction potentials for modeling the structure of benzene and the form of the radial and angular–radial distribution functions obtained. Table 1 systematizes the works devoted to the molecular dynamics modeling of the structure of liquid benzene [2–37].

Using the molecular dynamics method, a new technique at that time, the authors of [2–5] tried to gain insights into the structure of liquid benzene. The conclusions were drawn based on pair correlation functions, radial and angular. Note, however, that the six-center potentials used in [2–5] were not too accurate, although able to truthfully reproduce some thermodynamic properties of the liquid. Later, the focus was on constructing potentials that would provide a correct description of the thermodynamic properties of liquid benzene over a wide temperature range (Table 2) and the structure of the crystalline phase (Tables 3, 4). In addition, in a number of studies, the interaction potential was parameterized so as to make it suitable for describing the quantum-mechanically calculated geometry of gaseous benzene dimer. Using various model potential functions, the authors examined how the distribution functions depend on the temperature and how the computer simulation results vary with the number of species used in modeling.

In 1997, in addition to the pair correlation function, the radial-angular distribution function (RADF) came into use:

$$G(r, \theta) = \frac{1}{N\rho(r, \theta)}\left\langle \sum_i \sum_{j \neq i} \delta(r - r_{ij})\delta(\theta - \theta_{ij})\right\rangle,$$

which gives correlations for the pair of molecules i and j, the distance between the centers of mass of which is r_{ij} and the angle between the molecular planes is θ_{ij}; $\rho(r, \theta) = (N/V)2\pi r^2 \sin\theta \Delta r \Delta\theta$ is the number of molecules in the volume element. The shape of the RADF indicates the most probable configurations of the molecules. Since then, the structure of liquid benzene and the form of the corresponding RADF became virtually equivalent notions.

Characteristics of Interaction Potentials

In the first Monte Carlo (MC) and molecular dynamics (MD) studies of the structure of liquid benzene, the interaction of atoms (sites) was described by the six-center Lennard-Jones (6-12) potential,

$$U_{ij} = 4\varepsilon[(\sigma/r_{ij})^{12} - (\sigma/r_{ij})^6]$$

with and without a quadrupole potential situated at the center of the molecule.

The authors of [5] tested a six-center (6-12) potential with three sets of parameters. The calculated functions $g_{CC}(r)$, which characterize the probability of two carbon atoms being separated by a given distance, were compared to experimentally measured analogous functions [43]; it proved, however, difficult to favor any of the sets of parameters. This result led researchers to argue that the function $g_{CC}(r)$ is generally insensitive to

Table 1. A review of studies on the modeling of liquid benzene

Reference	Method	Molecule model	Potential	T, K	ρ, kg/m^3	N	Calculated values and functions
[2]	MC	6S	6-12 [3]	298	858	108	$g_{XX}(r)$, $g_{XS}(r)$, $g_{SS}(r)$, $\bar{\lambda}_i(r)$, $\bar{\lambda}_j(r)$, $\bar{\lambda}_{ij}(r)$
				328	821		
[4]	MD	6S	6-12 [3]	288	804	216	$g_{XX}(r)$, $g_{CC}(r)$, $g_{CH}(r)$, $g_{HH}(r)$, $D(t)$ $\langle\Phi_{00}^{202}\rangle$, $\langle\Phi_{00}^{220}\rangle$, $\langle\Phi_{00}^{224}\rangle$
[5]	MD	6S	6-12 [3]	301	874	64	$g_{XX}(r)$, $g_{CC}(r)$, $\bar{\lambda}_i(r)$, $\lambda_j(r)$, $\bar{\lambda}_{ij}(r)$
		6S (6C)	6-12 [5]	298			
		6S (6C)	6-12+Q [5]	302			
[6]	MC	6S	6-12 [6]	298	874	125	$g_{XX}(r)$, $g_{SS}(r)$, $\bar{\lambda}_i(r)$, $\lambda_j(r)$, $\bar{\lambda}_{ij}(r)$, $G(r, \theta)$
[7]	MC	6C + 6H	1-4-6-9-12 [8]	308	864	108	$g_{XX}(r)$, $g_{CC}(r)$, $g_{CH}(r)$, $g_{HH}(r)$, $g(r)$, $\bar{\lambda}_i(r)$, $\bar{\lambda}_j(r)$, $\bar{\lambda}_{ij}(r)$, $S(k)$
				348	819		
[9]	MD			312	819	108	$D(t)$, $c(t)$
				340	864		
[10]	MD	6C + 6H	6-exp [11] + U_{intra} [12]	305	874	32	$g_{XX}(r)$, $g_{CC}(r)$, $g_{CH}(r)$, $g_{HH}(r)$, D, S_s, $c(t)$, ω
[13]	MD	6S	6-12 [3]	280	~900		$g_{CC}(r)$, $U/nkT(T)$, $B(T)$, $c(T)$
		6S	6-12 [3]+Q [13]	…			
		6S (6C)	6-12 [3]	…		256	
		6S (6C)	6-12 [3]+Q [13]	…			
		$(x, y, z, \varphi, \theta)_{XX}$	6-12+Q+χ [13, 14]	460	~680		
[15]	MC	6S	6-exp+Q [15]	300	–	72	$g_{XX}(r)$, $g_{CC}(r)$, $g_{CH}(r)$, $g_{HH}(r)$
		6S	6-exp+Q [16]				$\langle\Phi_{00}^{202}\rangle$, $\langle\Phi_{00}^{220}\rangle$, $\langle\Phi_{00}^{224}\rangle$
		6C + 6H	6-exp+q [15, 17]				
[18]	MD	6S	6-12 [3, 5, 19]	298	874	72	U/nkT, p
			6-12+Q [5]				$g_{XX}(r)$, $\lambda_{ij}(r)$
			6-12 [20]				
[21]	MD	6S	6-12 [3, 5]	298	–	150	$g_{CC}(r)$, D, $B(T)$
		6S	6-12+Q [5]				
		6C + 6H	6-exp [22]				
		6C + 6H	6-exp+q [17, 21]				
[23]	MD	6C + 6H	6-exp+q [17, 25]	300	872	256	$g_{XX}(r)$, $g_{\text{inter}}(r)$, $G(r, \theta)$, $(d\sigma/d\Omega)_{\text{inter}}$, D
[24]							$g_{CC}(r)$, $g_{CH}(r)$, $g_{HH}(r)$
[26]	MD	6C + 6H	6-12 [27] + U_{intra} [28]	298	874	125	$g_{XX}(r)$, $D(T)$, $c(t)$
				323	848		
				353	816		
[29]	MC	$(x, y, z, \varphi, \theta, \psi)_{XX}$	6-12 [30]+ q [29]	298	519–635	512–608	$G(r, \theta)$
[31] [32]	MD	6C + 6H	6-12+q + U_{intra} [33]	298	873	500	$g_{XX}(r)$, $G(r, \theta)$, $(d\sigma/d\Omega)_{\text{inter}}$, $c(t)$, ω
			6-exp+q [34]	278	874		
			6-12+q [35]	298			
[36]	MC	$(x, y, z, \varphi, \theta)_{XX}$	6-12+Q+χ [37]	300	870	125	$g_{XX}(r)$, $g_{CC}(r)$, $G(r, \theta)$
						512	
						1024	

Note: MC and MD stand for the Monte Carlo and molecular dynamics methods, respectively. According to the six-site models, the benzene molecule can be represented by six force centers (sites), the positions of which can either coincide with the carbon atoms (6C) or not (6S). The 12-site model (6C + 6H) specifies the positions of the carbon and hydrogen atoms. The $(x, y, z, \varphi, \theta, \psi)_{XX}$ set indicates the coordinates of the centers of mass of the molecules (x, y, z) and the Euler angles φ, θ, ψ; $(x, y, z, \varphi, \theta)_{XX}$ indicates the mutual orientation of the molecules when the rotation of the molecules in the benzene ring plane is disregarded, since the benzene molecule is thought of as a disk. The description of the (6-12), (6-exp), (1-4-6-9-12) potentials is given in the text; the parameter χ in the potential describes the molecular anisotropy, U_{intra} is the intramolecular potential for nonrigid molecular models. The electrostatic interactions were taken into account through the quadrupole moment (Q) and point charges on the atoms (q). T is the temperature at which the modeling was performed; ρ is the density calculated at the required temperature ($\rho = 874$ kg/m^3 at 298 K [38]; N is the number of molecules used to performed the modeling; $g_{XX}(r)$, $g_{XS}(r)$, $g_{SS}(r)$, $g_{CC}(r)$, $g_{CH}(r)$, $g_{HH}(r)$ are the radial distribution functions for the distances between the centers of mass of the molecules, between the centers of mass of the molecules and the force centers (sites), between the sites, between the carbon atoms, between the carbon and hydrogen atoms, and between the hydrogen atoms; $\lambda(r)$ and Φ are the angular correlation functions; $G(r, \theta)$ is the radial–angular distribution function; $S(k)$ is the statistical structural factor, $(d\sigma/d\Omega)_{\text{inter}}$ is the coherent scattering cross section; S_s is the dynamic structural factor, $c(t)$ is the velocity autocorrelation function; D, $D(t)$ is the self-diffusion coefficient; $B(T)$ is the second virial coefficient; and ω is the frequency of harmonic vibrations.

Table 2. Thermodynamic characteristics of liquid benzene calculated at 298–300 K

Potential	$-U_{\text{int}}$, kJ/mol	$-U_{\text{int}}/nkT$, kJ/mol	p, MPa
6-12 [3]	29.0 [4] 33.7 [21] 34.2 [6]	57.0 [5] 54.9 (58.7) [18]	230.0 [21] 100.6 (21.8) [18]
6-12 [5]	31.3 [21]	52.8 [5]	–7.0 [21]
6-12+Q [5]	31.3 [21]	52.8 [5]	1.0 [21]
6-12 [6]	32.3 [6]	–	6.0 [6]
6-exp+Q [15]	32.3 [15]	–	–
6-exp+q [16]	34.8 [15]	–	–
6-exp+q [17]	34.7 [15] 36.2 [21]	–	150.0 [21]
6-12 [19]	–	42.7 (46.1)	20.7 (–51.4) [18]
6-12 [20]	–	51.1 (54.4)	61.6 (–21.3) [18]
6-12+q [21]	31.8 [21]	–	–7.0 [21]
6-exp [22]	27.0 [21]	–	75.0 [21]
6-exp+q [34]	–	–	0.1 [32]
6-12+q [35]	–	–	0.05 [32]
Experiment	31.0 [39] 31.94 [6]	53.2 [39]	0.1 [39]

Note: In [4], the calculations were performed at 288 K with the potential borrowed from [3]. Parenthesized are the values adjusted so as to include the potential cutoff corrections obtained in [18].

Table 3. Description of the properties of the orthorhombic modification of crystalline benzene at a pressure of 0.1 MPa

Potential	V, Å^3	a, Å	b, Å	c, Å	θ, deg	φ, deg	ψ, deg	T, K
6-12 [3]	513.4	7.1	10.3	7.0	47.3	0.0	90.1	0
6-12 [5]	470.4	7.1	9.5	7.00	47.3	0.0	90.1	0
6-12+Q [5]	460.0	7.0	9.7	6.8	46.3	0.0	90.1	0
1-4-6-9-12 [8]	399.0	7.2	8.7	6.4	45.9	22.9	87.7	0
6-exp+Q [16]	501.6	6.9	10.9	6.7	–	–	–	218
6-exp+q [17]	511.2	7.3	9.8	7.2	–	–	–	218
6-exp+Q [15]	525.2	7.5	10.2	6.9	–	–	–	218
6-exp [22]	481.2	7.4	9.4	6.9	44.9	21.4	86.6	135
I	491.6	7.4	9.6	6.9	–	–	–	218
II	443.3	7.3	9.2	6.6	45.8	24.1	86.6	0
III	448.0	7.3	9.2	6.6	40.9	22.8	88.9	0

Note: θ, φ, and ψ are the angles that specify the orientation of a molecule in the cell [40]; (**I**) experimental results obtained at an external pressure of 70 MPa, (**II**) experimental values extrapolated to 0 K, and (**III**) experimental values extrapolated to 0 K and rescaled [41].

Table 4. Description of the properties of the monoclinic modification of crystalline benzene at 2.5 MPa and 294 K

Potential	V, Å^3	a, Å	b, Å	c, Å	α, deg	β, deg	γ, deg
6-exp+Q [16]	199.0	5.20	5.72	7.02	90.0	107.6	90.2
6-exp+q [17]	207.2	5.34	5.31	7.71	89.8	107.9	90.1
6-exp+Q [15]	203.6	5.45	5.43	7.35	89.8	110.7	90.0
Experiment [42]	206.4	5.42	5.38	7.35	90.0	110.0	90.0

the form of the potential. Nevertheless, calculations of the energetic characteristics of the monoclinic and orthorhombic modifications of crystalline benzene demonstrated that the model that included the quadrupole potential gave a better description, a result that led the authors to conclude that the modeling of the properties of condensed benzene should allow for electrostatic interactions.

The authors of [8] proposed a (1-4-6-9-12) intermolecular potential composed of electrostatic, induction, and dispersion terms:

$$U = \sum [A_i r_i^{-1} + B_i r_i^{-4} + C_i r_i^{-6} + D_i r_i^{-9} + E_i r_i^{-12}].$$

Here, A, B, C, D, and E are constants; the summation is performed over all C–C, C–H, and H–H interactions. This potential closely reproduced the geometry of benzene dimers, parameters of the unit cell, and the orientation of the molecules in crystalline benzene. In [7, 9], the (1-4-6-9-12) potential was used to calculate the characteristics of liquid benzene by the MC and MD methods. A serious drawback of this potential is that it involves a large number of site–site interactions, a feature that forced the authors to introduce an isotropic potential at distances longer than 10 Å. In addition the (1-4-6-9-12) potential proved to be incapable of describing compounds other than benzene because of the inapplicability of the standard procedures of mixing to its parameters.

Some researchers modeled liquid benzene with the use of the Buckingham (6-exp) potential:

$$U_{ij} = A_{ij} \exp(-B_{ij} r_{ij}) - C_{ij} r_{ij}^{-6}.$$

In many studies, this potential was modified so as to include the term describing the Coulomb interaction of quadrupole (6-exp+Q) or point (6-exp+q) charges.

The (6-exp+q) potential with the parameters proposed in [17, 22, 25] was found to closely reproduce the properties of the crystalline phases of benzene. In addition, it proved suitable for studying the properties of benzene in passing from normal to supercritical conditions [24]. This potential can be thought of as a 12-center potential the interaction sites of which coincide with the carbon atoms, while the protons are somewhat shifted to the carbon atoms so as to ensure a better description of the electron density distribution. The values of the point charges on each of the atoms are adjusted so at to reproduce the quadrupole moment as closely as possible. Note also that the C···H-interaction parameters can be calculated from the C···C and H···H interaction parameters by using the standard procedures of mixing. What is more, the parameters determined in this way are applicable to other classes of compounds.

The authors of [21] proposed a (6-exp+q)-type potential capable of describing the thermodynamic properties of benzene over a wide temperature range. They demonstrated that this potential reproduces the results of the quantum-mechanical calculations of the benzene dimer characteristics reported in [39]. Note, however, that the question of whether this potential can be successfully applied to modeling the liquid phase remains open, since, along with predicting the thermodynamic properties (which can be closely described with the use of other potentials as well (Table 2)), the authors of [21] calculated only the self-diffusion coefficient and the function $g_{\mathrm{CC}}(r)$, which, as follows from the discussion in [5] and from the published data we looked through, is virtually insensitive to the form of the potential. In addition, the parameterization of the potential intended for determining the properties of the liquid phase on the basis of quantum-mechanical calculations seems questionable, since a liquid system cannot be treated as a rarefied gas, and, additionally, more refined ab initio calculations of the geometric and energetic characteristics of the benzene dimer [44] disprove the previous results.

Given that the benzene molecule exhibits well-pronounced spatial anisotropy, the authors of a number of works used an anisotropic version of the (6-12) potential. In particular, the Gay–Berne potential [14] allows for the dependence of the σ and ε parameters on the mutual orientation of and distance between the molecules. When studying liquid benzene, the authors of [13] added a quadrupole interaction term to the Gay–Berne potential, a term that also depended on the distance between and mutual orientation of the molecules. This potential was used to study the thermodynamic properties of liquid benzene. Unfortunately, little attention was paid to the structural characteristics; therefore, the above comment refers to this work as well. In [36], an additional parameterization of the Gay–Berne was performed so as to make it more effective in describing the benzene dimer.

Structural Characteristics of Liquid Benzene

The discussion of the structure of liquid benzene in all the works reviewed (Table 1) is limited to an analysis of the form of the correlation functions, with the assumption made in many cases that the arrangement of the molecules in the liquid phase is much the same as in the solid phase [2, 31, 45]. The authors of [2] compared the function $g_{\mathrm{XX}}(r)$ with the relative histogram of the crystal at 138 K (Fig. 1). The histogram shows the positions of molecules corresponding to the nearest-neighbor environment in the crystal. The parameters of the crystallographic cell were rescaled by reducing the cell volume to the value obtained from numerical experiments. Comparing the histograms and $g_{\mathrm{XX}}(r)$, the authors concluded that the packing of molecules in the liquid state is very similar to that observed in the solid state; in particular, the distribution function shows that the principal structural features are located at positions corresponding to those indicated in the histogram. Analyzing the orientational correlations in the liquid, the authors revealed that, at 5.4 Å, the molecules are ori-

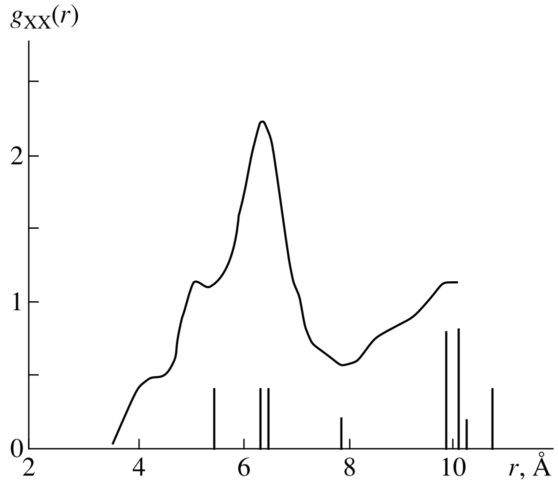

Fig. 1. Compares the function $g_{XX}(r)$ at 298 K with the positions of the molecules in a rescaled crystal cell (vertical lines), according to the data from [2].

ented perpendicular to each other, an observation that led them to conclude that not only the relative positions, but also mutual orientations, of the molecules in the liquid state correspond to those in the solid state.

In [31], the distribution functions for the liquid state were compared to the positioning of individual molecules in the crystal. As a result, a $g_{XX}(r)$ function was obtained, the form of which, in authors' opinion, suggest the existence of a well-pronounced cellular structure around each molecule (Fig. 2). To estimate the size of the shells, the authors calculated the distribution of distances from a singled-out molecule to 12 molecules in its nearest environment. The results are displayed in Fig. 3. The authors believe that this comparison shows that the cells in the liquid and crystal are similar, although a significant scatter of the distances is observed. The authors believe that the main distinction between the two phases is the absence of any preferrable orientation in the nearest environment of the molecules in the liquid.

In [5], stack-shaped configurations were observed at small distances, a result that led the authors to conclude that there is no preferrable orientations of molecules in liquids. Note, however, that modeling with the use of the six-site (6-12) potential in earlier works, [2, 4–6], predicted a marked increase in the fraction of stack-shaped configurations in the nearest environment of the molecules, as can be seen from the shoulder (maximum) in the $g_{XX}(r)$ function at a distance of ~4 Å (Fig. 1); calculations based on more refined forms of the potential normally show no such features (Fig. 2). Note also that the sizes of the regions of correlation of the radial distribution functions reported in the different works differ (in earlier works, it was 10 Å (Fig. 1); in later studies, it extended to up to 15–18 Å (Fig. 2)), which may be explained by the form of the potential.

The RADF obtained in [31] (Fig. 4) suggests that, in the liquid, unlike in the crystal, the number of perpendicular orientations only 1.5 times that of parallel ones. The authors established that the ratio between perpendicular and parallel orientations in the nearest environment of the molecules remains unchanged as the charges on the atoms are increases from 0.115 to 0.151 e; i.e., as the quadrupole moment increases, the fraction of perpendicular orientations remains essentially the same. This observation suggests that the existence of parallel orientations in the nearest environment of molecules is a remarkable property of the liquid phase. Later, these

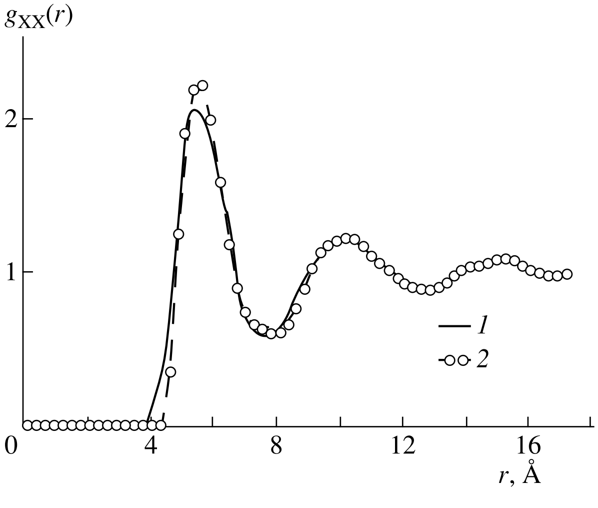

Fig. 2. Functions $g_{XX}(r)$ calculated by the (*1*) molecular dynamics [31] and (*2*) Monte Carlo methods [36].

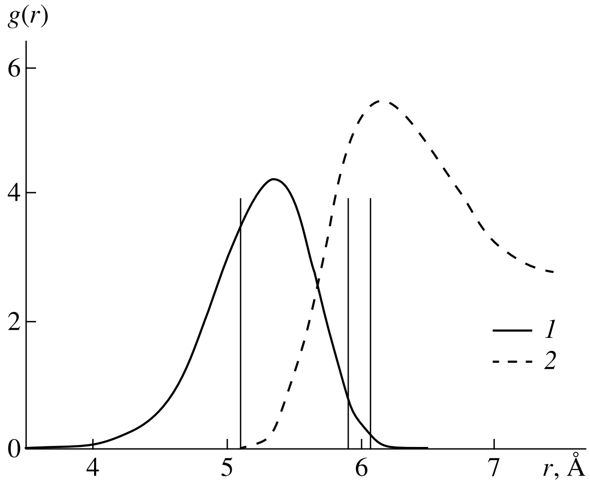

Fig. 3. Mean distance between the molecules in the cell of the liquid: (*1*) the first (composed of four molecules) and (*2*) the second (eight molecules) coordination spheres. The vertical lines indicate the positions of the 12 molecules constituting the nearest environment of a molecule in the crystal. According to the data from [31].

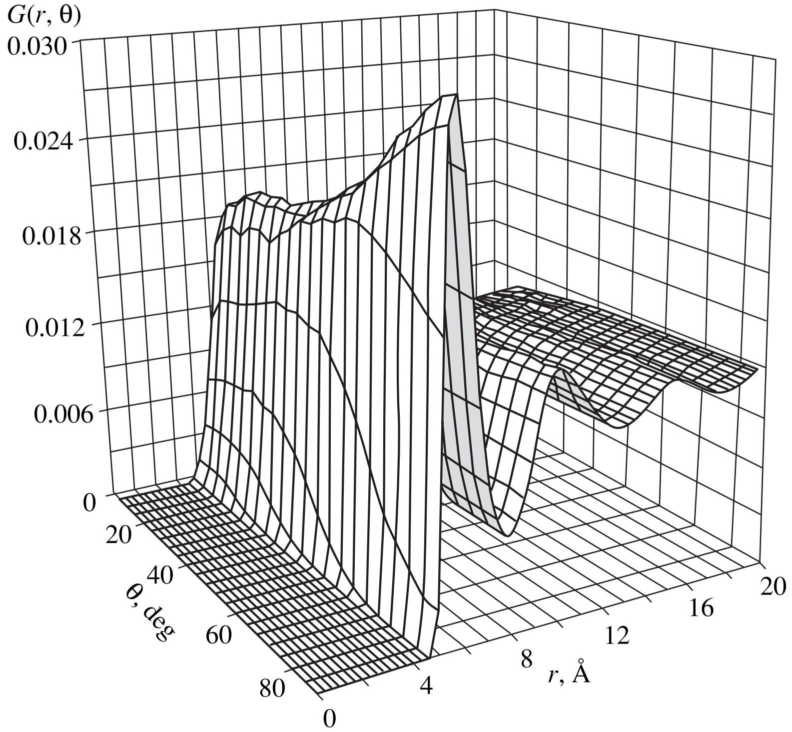

Fig. 4. Radial-angular distribution function for benzene at 298 K [31].

conclusions were supported by calculations with other model potentials [32].

According to the RADFs plotted in [23, 24, 36], the orientation of the nearest environments of the molecules is random. Comparing the distribution functions obtained by the different authors, one can see that their shapes are identical at distances longer than 4–5 Å, with distinctions arising within a shorter range. In particular, it was found [23, 31, 32] that perpendicular orientations are slightly preferrable at short distances. This can be attributed to the fact that the potential used was parameterized so as to describe the properties of the gaseous benzene dimer, for which the stack-shaped configurations have a higher energy than the T-shaped ones [44, 46]. The authors of [36] reported a marked increase in the fraction of parallel orientations within the range of 4.5–4.7 Å.

Thus, an analysis of the results of the molecular dynamics modeling of liquid benzene led us to the following conclusions.

(1) Nearly all existing potential functions closely reproduce the experimentally measured thermodynamic and dynamic characteristics of liquid benzene; at the same time, many potential functions used to model the properties of liquid benzene satisfactorily describe the properties of the crystalline state and the geometry of the benzene dimer in the gas phase.

(2) The six-site potentials without electrostatic interaction terms overestimate the fraction of stack-shaped configurations in the nearest environment of the molecules and, consequently, have only a limited applicability.

(3) Increasing the number of molecules used in modeling (from 125 to 1024) and making the molecule rigid or flexible produce only a small effect on the energetic characteristics and the shape of the correlation functions.

(4) The existence of stack-shaped configurations in the nearest environment of the molecules in liquid benzene is a distinctive feature of the liquid phase as compared to the crystalline phase.

(5) The radial distribution function $g_{XX}(r)$ at 298 K is indicative of the existence of correlations in the liquid up to distances of 15–18 Å, with the maxima of these functions being located at ~6, ~10, and ~15 Å.

(6) An analysis of the RADF is indicative of an almost random angular distribution, with the answer to the question whether the perpendicular or parallel orientation is slightly predominant at short distances (≤4.5–4.7 Å) being dependant on the parameterization of the potential function.

(7) The radial distribution function $g_{CC}(r)$ yields too little information on the structural peculiarities of the liquid and is virtually insensitive to the form of the potential function.

(8) As the temperature increases, the maxima of the radial distribution function smear while retaining their positions.

Thus, the main conclusions on the structure of liquid benzene that can be drawn from distribution functions are that, unlike the crystalline phase, the liquid phase contains parallel-orientated molecules at short distances and that, at longer distances, random mutual orientations of molecules are observed. This conclusion is true irrespective of the form of the potential function, which may correctly describe macroscopic characteristics of the system but provide little information on the structure of the liquid (when treated based on the correlation functions). Only slightly dependent on the form of the potential, the averaged characteristics derived from the correlation functions do not reflect the actual structure of the liquid.

ACKNOWLEDGMENTS

This work was supported by the Russian Foundation for Basic Research, project no. 05-03-32946.

REFERENCES

1. G. A. Martynov, Zh. Strukt. Khim. **43** (3), 547 (2002).
2. D. J. Evans and R. O. Watts, Mol. Phys. **32**, 93 (1976).
3. D. J. Evans and R. O. Watts, Mol. Phys. **31**, 83 (1976).
4. O. Steinhauser, Chem. Phys. **73**, 155 (1982).
5. M. Classens, M. Ferrario, and J.-P. Ryckaert, Mol. Phys. **50**, 217 (1983).
6. F. S. Adan, A. Banon, and J. Santamaria, Chem. Phys. **86**, 433 (1984).
7. P. Linse, J. Am. Chem. Soc. **106**, 5425 (1984).
8. G. Karlstrom, P. Linse, A. Wallqvist, and B. Jonsson, J. Am. Chem. Soc. **105**, 3777 (1983).
9. P. Linse, S. Engstrom, and B. Jonsson, Chem. Phys. Lett. **115**, 95 (1985).
10. J. Anderson, J. J. Ullo, and S. Yip, J. Chem. Phys. **86**, 4078 (1987).
11. B. M. Powell, G. Dolling, and H. Bonadeo, J. Chem. Phys. **69**, 2428 (1978).
12. P. Pulay, G. Fogarasi, and J. E. Boggs, J. Chem. Phys. **74**, 3999 (1981).
13. S. Gupta, W. B. Sediawan, and E. McLaughlin, Mol. Phys. **65**, 961 (1988).
14. J. G. Gay and B. J. Berne, J. Chem. Phys. **74**, 3316 (1981).
15. S. Yashonath, S. L. Price, and I. R. McDonald, Mol. Phys. **64**, 361 (1988).
16. S. L. Price and A. J. Stone, J. Chem. Phys. **86**, 2859 (1987).
17. D. E. Williams and S. R. Cox, Acta Crystallogr., Sect B: Struct. Sci. **40**, 404 (1984).
18. A. Baranyai and D. J. Evans, Mol. Phys. **70**, 53 (1990).
19. D. J. Evans and R. O. Watts, Mol. Phys. **32**, 995 (1976).
20. C. Hoheisel, J. Chem. Phys. **89**, 7457 (1988).
21. G. D. Smith and R. L. Jaffe, J. Phys. Chem. **100**, 9624 (1996).
22. D. E. Williams and T. L. Starr, Comput. Chem. **1**, 173 (1977).
23. M. I. Cabaco, Y. Danten, M. Besnard, et al., J. Phys. Chem. B **101**, 6977 (1997).
24. T. Tassaing, M. I. Cabaco, Y. Danten, and M. Besnard, J. Chem. Phys. **113**, 3757 (2000).
25. D. E. Williams and D. J. Houpt, Acta Crystallogr., Sect. B: Struct. Sci. **42**, 286 (1986).
26. T. Nakagawa, S. Yamanaka, H. Urakawa, et al., THEOCHEM **458**, 275 (1999).
27. A. Maliniak and A. Laaksonen, Mol. Phys. **62**, 489 (1987).
28. P. C. Painter and R. G. Snyder, Spectrochim. Acta, Part A **36**, 337 (1980).
29. P. M. Zorkii, E. V. Sokolov, G. G. Malenkov, and L. V. Lanshina, Zh. Fiz. Khim. **74**, 195 (2000) [Russ. J. Phys. Chem. **74**, 177 (2000)].
30. V. B. Zhurkin, V. I. Poltev, and V. I. Florenskii, Mol. Biol. **14**, 1116 (1980).
31. R. Chelli, G. Cardini, P. Procacci, et al., J. Chem. Phys. **113**, 6851 (2000).
32. R. Chelli, G. Cardini, M. Ricci, et al., Phys. Chem. Chem. Phys. **3**, 2803 (2001).
33. B. R. Brooks, R. E. Bruccoleri, B. D. Olafson, et al., J. Comput. Chem. **4**, 187 (1983).
34. S. Califano, R. Righini, and S. H. Walmsley, Chem. Phys. Lett. **64**, 491 (1979).
35. W. L. Jorgensen and D. L. Severance, J. Am. Chem. Soc. **112**, 4768 (1990).
36. S. Lorenz, T. R. Walsh, and A. P. Sutton, J. Chem. Phys. **119**, 2903 (2003).
37. R. Berardi, C. Fava, and C. Zannoni, Chem. Phys. Lett. **236**, 462 (1995).
38. *CRC Handbook of Chemistry and Physics* (CRC, Boca Raton, FL, 1997–1998).
39. F. D. Rossini, K. S. Pitzer, R. L. Arnett, et al., *Selected Values of Physical and Thermodynamic Properties of Hydrocarbons and Related Compounds*, Am. Petr. Inst. Res. Pr. 44 (Carnegie Press, Pittsburgh, PA, 1953).
40. K. C. Janda, J. C. Hemminger, J. S. Winn, et al., J. Chem. Phys. **63**, 1419 (1975).
41. X. Shi and L. S. Bartell, J. Phys. Chem. **92**, 5667 (1988).
42. G. E. Bacon, N. A. Curry, and S. A. Wilson, Proc. R. Soc. London, Ser. A **279**, 98 (1964).
43. A. H. Narten, J. Chem. Phys. **48**, 1630 (1968).
44. M. O. Sinnokrot, E. F. Valeev, and C. D. Sherrill, J. Am. Chem. Soc. **124**, 10887 (2002).
45. B. Ratalska-Gadomska, W. Gadomski, P. Wiewior, and C. Radzewicz, J. Chem. Phys. **108**, 8489 (1998).
46. P. Hobza, H. L. Selzle, and E. W. Schlag, J. Am. Chem. Soc. **116**, 3500 (1994).